Study of the light-induced metal-insulator transition in $SrTiO_3$ by photoresistance spectroscopy

G. Bridoux,[1,2,*] M. Villafuerte,[1,2] J. M. Ferreyra,[1] N. Bachi,[1] C. A. Figueroa,[1] and S. P. Heluani[1]

[1] *Laboratorio de Física del Sólido, Facultad de Ciencias Exactas y Tecnología, Universidad Nacional de Tucumán, 4000 Tucumán, Argentina*

[2] *Consejo Nacional de Investigaciones Científicas y Técnicas - CONICET, Argentina*

(Dated: September 18, 2015)

Photoresistivity and its spectral response has been systematically studied in oxygen deficient $SrTiO_3$ single crystals for a wide range of resistivities, ρ, and carrier densities, n. At room-temperature we have found a persistent photoresistance that gradually decreases as ρ is diminished or n is increased in addition to relaxation times of seconds to a few minutes suggesting that trapping of carriers is playing a major role. An analysis of the photoresistance excitation spectra shows two distinctive features that are related to the indirect gap of $SrTiO_3$ at (3.25 ± 0.04) eV and to a direct transition at (3.40 ± 0.03) eV. The photoresistive crystals present a temperature dependent resisitivity under illumination that experiences a metal-insulator transition below $T \sim 85$ K. Low-temperature photoresistance spectrum reveals as a suitable technique to understand the origin of this transition, pointing to an enhanced efficiency of the ~ 3.25 eV gap to promote electrons to the bottom of the conduction band.

$SrTiO_3$ (STO) is the building block for many of the functional oxide thin films grown nowadays and a suitable platform for the development of oxide-based electronics [1, 2]. It is well established that STO is a band gap insulator with an indirect gap of $3.2 - 3.27$ eV [3, 4] but it also experiences direct transitions like the $X_{5'} \rightarrow X_3$ at 3.46 eV observed in optical absorption experiments [4]. Although during the 60's this material was studied by several groups, in the last decade there has been a renewed interest on STO due to the discovery of a high mobility 2D electron gas at the interface of the bilayer $LaAlO_3/SrTiO_3$ [5–7] in which photoresistivity has been reported [8, 9]. Photoresistivity on bulk STO is known since the pioneering work of Yasunaga *et al.* [10] but not enough attention has been paid to it up to the recent work of Tarun *et al.*[11]. These authors have remarkably found photoresistivity with a permanent effect in Strontium enriched STO single crystals where the generated Ti vacancies seem to play an important role on this effect [11]. Even though permanent photoresistance is an appealing ingredient for information storage devices it might be not required in the design of optoelectronic devices where photoresistivity with faster relaxation times is needed [12].

$SrTiO_3$ can be easily doped with electrons by means of oxygen vacancies generation [13] produced with a simple thermal annealing in vacuum. In this way, carrier density, n, can be increased in several orders of magnitude, filling the first band of STO and reaching the metallic state [14]. This powerful and simple procedure led, for example, to the discovery of superconductivity on STO for $n \gtrsim 5.5 \times 10^{17}\,\mathrm{cm^{-3}}$ below 86 mK [15, 16]. Following this technique and knowing the relevance that oxygen vacancy defect-levels inside the gap can have in the optical and optoelectronic properties of oxide semiconductors [17, 18], we present a systematic photoresistance study on several thermal annealed $SrTiO_3$ single crystals with different room-temperature resistivities and carrier concentrations ranging from $1.7 \times 10^8\,\Omega\,\mathrm{cm}$ to $1.5\,\Omega\,\mathrm{cm}$ and $n < 10^{11}\,\mathrm{cm^{-3}}$ to $1.4 \times 10^{18}\,\mathrm{cm^{-3}}$ respectively. At room temperature we have found persistent photoresistance with a value of $\sim 33\%$ for the crystal with $1.7 \times 10^8\,\Omega\,\mathrm{cm}$, and it gradually decreases as resistivity is diminished and carrier concentration increased, up to become negligible in the low resistive metallic state. In addition, the temporal response of seconds to a few minutes has been explained in terms of deep-level traps generated by Ti-O vacancy pairs. The photoresistance excitation spectrum reveals a fingerprint of the indirect gap at ~ 3.25 eV but also of a direct transition at ~ 3.40 eV. To conclude, a metal-insulator transition induced by light has been observed in the temperature dependent resistivity at $T \sim 85$ K, linked to an improvement of the photoelectron generation of the ~ 3.25 eV gap, as confirmed by low-temperature photoresistance spectra.

For this study, commercial (100) $SrTiO_3$ single crystals like those used in previous studies [19, 20] were annealed at a fixed temperature between 550 and 800°C during 30 min at 10^{-7} Torr in order to produce a n-type doping on these crystals [16, 20]. Oxygen diffusion coefficients [21–23] of $D \approx 10^{-5}$-$10^{-6}\,\mathrm{cm^2 s^{-1}}$ warranty a reduction in the whole volume (2.5 mm $\times$ 2.5 mm $\times$ 0.5 mm) of the STO single crystals. Ohmic contacts with linear and symmetric $I - V$ curves were achieved by using sputtered Au pads on the STO crystals. Resistivity and Hall effect measurements were performed in a current source-nanovoltmeter configuration while for high resistivity measurements (above $10^5\,\Omega\,\mathrm{cm}$) a voltage source-ammeter configuration was more appropriate. In the latter case, an excitation voltage of 5 V was used and the electrical current was measured with a resolution of ~ 0.5 nA. Measurements were carried out in a

* gbridoux@herrera.unt.edu.ar

standard cryostat equipped with an optical window, a 1000 W Xe lamp plus a monochromator (applied incident light from 200 to 800 nm with an estimated flux density of $\sim 10\,\mathrm{mW\,cm^{-2}}$) and an electromagnet (magnetic fields up to 0.85 T).

At room-temperature, the typical behavior of the time dependent photoresistivity (defined as $PR = (\rho - \rho_{dark})/\rho_{dark})$) is presented in Figure 1 for three crystals with different resistivities in the dark (without illumination), ρ_{dark}. As it can be noticed, the photoresistance is higher for the samples with higher resistivities, reaching a value of 33% for the crystal with $\rho_{dark} = 1.7\times10^{8}\,\Omega\,\mathrm{cm}$. Table I summarizes the properties at room-temperature of the different STO crystals studied in this work and it confirms that photoresistance starts to decrease when n is increased (and ρ is diminished) up to become negligible within our experimental uncertainty for samples deep into the metallic state [14].

The decrease of photoresistance when the carrier density is increased can be explained assuming that the photocurrent $PC = \triangle I/I_0$ is proportional to $\triangle n/n_0$, where n_0 is the carrier density without illumination and $\triangle n$ is the variation of carrier density due to the illumination. The ratio of PC's between the sample with $n_0 = 4\times10^{11}\,\mathrm{cm^{-3}}$ and the one with $n_0 = 1\times10^{12}\,\mathrm{cm^{-3}}$ under the mentioned hypothesis and assuming that $\triangle n$ is the same for both samples, gives a calculated value of 2.5, which is not far from $\simeq 4$ obtained directly from the experimental PC values of these samples ($PC \simeq 7.6\times10^{-3}$ for the crystal with $n_0 = 4\times10^{11}\,\mathrm{cm^{-3}}$ and $PC \simeq 1.77\times10^{-3}$ for the one with $n_0 = 1\times10^{12}\,\mathrm{cm^{-3}}$).

The photocurrent growth and decay curves at room-temperature are shown in Fig. 2a and Fig. 2b respectively. While the main panels of Fig. 2a and Fig. 2b present the data for the sample labeled as S1, the respective insets show the curves corresponding to the crystal S2. At first glance, it can be noticed that higher values of relaxation times are obtained for crystals with higher photocurrents, which is in agreement with the proportionality between photocurrent and relaxation time in a photoresistive semiconductor [24]. Several trial functions like a stretch exponential [9] or a power-law decay [24, 25] have been tested to fit our curves without satisfactory results in all the measured range, but our data can be well described by two characteristic relaxation times whose values are estimated fitting a sum of two exponentials [24, 26–28], see Fig. 2. The resulting relaxation times are $\tau_1 \simeq 60\,\mathrm{s}$ and $\tau_2 \simeq 1100\,\mathrm{s}$ for the sample S1 and $\tau_1 \simeq 10\,\mathrm{s}$ and $\tau_2 \simeq 200\,\mathrm{s}$ for sample S2. In the case of the STO crystal labeled as S3 the fitting gives $\tau_1 \simeq 3\,\mathrm{s}$ and $\tau_2 \simeq 40\,\mathrm{s}$, hence the ratio τ_2/τ_1 remains approximately the same for all the crystals that present photoresistance.

It is well established that these relaxation times of seconds to a few minutes implies that trapping centers are playing an important role in the photocurrent decaying curves [24]. The location of these level-defects relative to the minimum of the conduction band can be estimated by $E_t \simeq k_B.T.\ln(\nu.\tau)$. Using the obtained relaxation times and an attempt to escape frequency of $\nu \simeq 5\times10^{12}\,\mathrm{s^{-1}}$ [24] it gives $E_t \sim 0.76 - 0.9\,\mathrm{eV}$ below the bottom of the conduction band. Some theoretical works [18, 29] propose that these deep-levels are originated by oxygen vacancies, V_O, resulting from the hybridization of Ti $3d$ and O $2p$ states and experimental evidence of mid-gap states at $\sim 1\,\mathrm{eV}$ below the minimum of the conduction band has been found by means of x-ray absorbtion spectroscopy (XAS) [30] and soft x-ray resonant photoemission spectroscopy (PES) [31]. On the other side, according to theoretical calculations [32], a more complex defect based on a Ti-O vacancy pair, V_{Ti-O}, which has a very low formation energy in reduced STO crystals can also generate deep-levels which are very efficient as carrier-trapping as

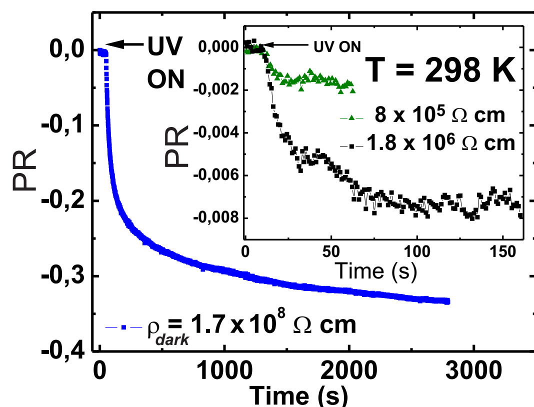

FIG. 1. Photoresistivity (defined as $(\rho - \rho_{dark})/\rho_{dark}$) as a function of the time for the sample with $\rho_{dark} = 1.7\times10^{8}\,\Omega\,\mathrm{cm}$ at $T = 298\,\mathrm{K}$. The applied incident wavelength was $\lambda = 365\,\mathrm{nm}$ ($\sim 3.40\,\mathrm{eV}$). The inset shows the corresponding photoresistance for the samples with $\rho_{dark} = 1.8\times10^{6}\,\Omega\,\mathrm{cm}$ (black squares) and $\rho_{dark} = 8\times10^{5}\,\Omega\,\mathrm{cm}$ (green triangles).

TABLE I. Room temperature ($T = 298\,\mathrm{K}$) properties of the annealed STO single crystals studied in this work. The first column presents the resistivity values of the different crystals (without illumination), the second column shows the corresponding carrier densities (without illumination) extracted from the Hall effect measurements and the third one the corresponding percent photoresistivity, defined as $(\rho - \rho_{dark})\times100/\rho_{dark}$.

ρ_{dark} [Ω cm]	n_0 [cm^{-3}]	PR [%]	Sample
1.7×10^{8}	$<1\times10^{11}$	33.0	S1
1.8×10^{6}	4×10^{11}	0.8	S2
8.0×10^{5}	1×10^{12}	0.1	S3
96.4	2×10^{16}	[a]	S4
10.6	1×10^{17}	[a]	S5
1.5	1.4×10^{18}	[a]	S6

[a] Photoresistivity was not observed.

confirmed by positron-annihilation spectroscopy (PAS) studies on STO [11, 33]. Furthermore, it should be considered that STO single crystals contain iron impurities and several experiments corroborate the presence of deep-levels generated by a Fe-V_O complex [34, 35]. From the above discussion, pre-established V_{Ti} or defects produce efficient trapping centers when they combine with a moderate concentration of V_O [11] resulting in higher relaxation times like in sample S1, see Fig. 2. As V_O concentration increases exceeding the pre-established V_{Ti} density, the V_{Ti-O} vacancy pairs traps with a -2 charge state are somehow screened by the $+2$ V_O, lowering in this way the trapping effect and the relaxation time for samples with higher carrier concentration like crystals S2 and S3, see Table I and Fig. 2.

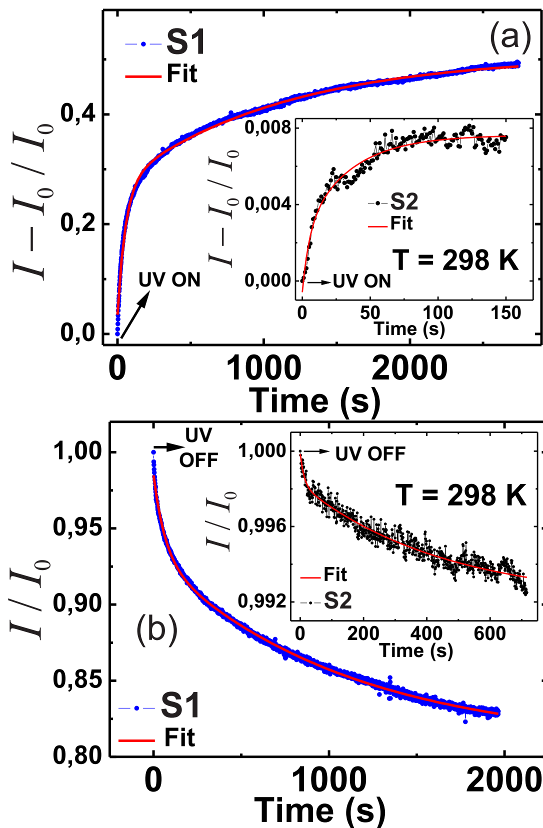

FIG. 2. a) Time evolution of electrical current, I, (normalized at its initial value I_0) during the application of an incident light of $\lambda = 365\,\mathrm{nm}$ for the sample S1 at $T = 298\,\mathrm{K}$. The data are well fitted by a two exponential decaying function (red line). The inset shows the corresponding data and fit for the sample S2. b) Time dependence of electrical current, I, (normalized at its initial value I_0) after an applied incident light of $\lambda = 365\,\mathrm{nm}$ was removed (sample S1 at $T = 298\,\mathrm{K}$). Again, the data are well fitted by a two exponential decaying function (red line). The inset shows the corresponding data and fit for the sample S2. Other trial functions have been tested to fit our data without succeed.

On the other hand, in resemblance with other indirect gap semiconductors [36] in STO one could ascribe the slow time response, τ_2, to an indirect gap transition assisted by a phonon [37], while the fast time response, τ_1, would be caused by a direct transition. If each one of these relaxation times are affected by similar time-delay caused by the same type of deep-level traps, the ratio τ_2/τ_1 should have the same value for all the photoresistive crystals which is in agreement with our observations. That is, while τ_1 and τ_2 are still dependent of the trapping process, the ratio τ_2/τ_1 is not and it only contains detailed information about the parameters involved in the transition probabilities for the indirect and direct processes [36]. The previous description is supported by the photoresistance excitation spectrum, depicted in Fig. 3 at $T = 110\,\mathrm{K}$ for the crystal S3, but its behavior is representative of the other crystals in the range between $T \simeq 85\,\mathrm{K}$ and room-temperature. The scanning speed of the incident light wavelength was $0.1\,\mathrm{nm\,s^{-1}}$ but lower scanning speeds led to the same results. Fig. 3a shows a sweep from low to higher energies (which we denote as L-H scan). At energies below the indirect gap of STO, the resistivity remains nearly constant due to the

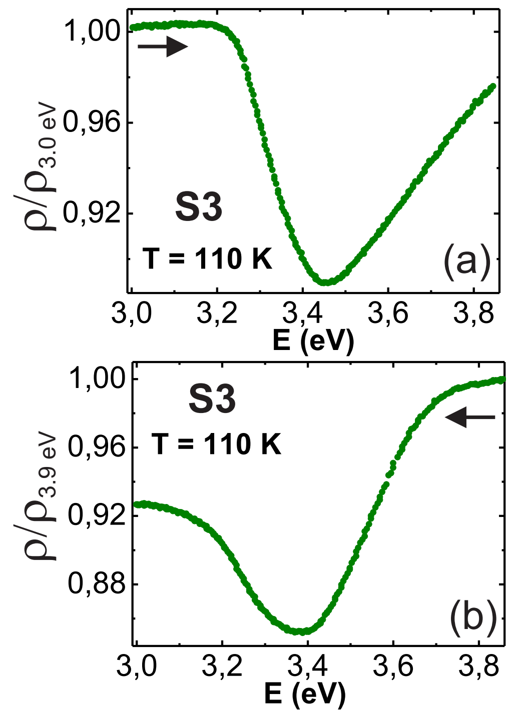

FIG. 3. a) Resistivity (normalized at its 3.0 eV value) as a function of the incident light energy for the sample S3 at $T = 110\,\mathrm{K}$. The arrow marks the direction of the scan (denoted as L-H scan). The maximum slope is reached at (3.25 ± 0.04) eV. b) Resistivity (normalized at its 3.9 eV value) as a function of the incident light energy for the same sample at $T = 110\,\mathrm{K}$. The arrow marks the direction of the scan (denoted in this case as H-L scan). A minimum is reached at (3.40 ± 0.03) eV.

absence of efficient states that can produce a significant promotion of electrons to the minimum of the conduction band. When the indirect gap energy is reached, a drop in the resistivity occurs, whose maximum slope value is (3.25 ± 0.04) eV. If energy is subsequently increased up to values above any efficient transition, the recombination rate starts to dominate, a minimum is reached and eventually resistivity starts to increase, see Fig. 3a. At this point, we perform a scan from high to lower energies (which we denote as H-L scan), see Fig. 3b. As can be observed, resistivity starts to decrease when energy is diminished, which is concomitant with the high energy regime of the previous L-H scan. A minimum is attained at (3.40 ± 0.03) eV, which is related with a direct $X_{5'} \rightarrow X_3$ transition in agreement with optical absorption experiments [4]. If energy is subsequently decreased from this value, the recombination rate starts to dominate and resistivity increases. In this situation, the efficiency of the 3.25 eV indirect gap to generate photoelectrons is low enough and it can not avoid this increment of resistivity. Our results are summarized in the energy diagram sketch of Fig. 4.

The performance of the resistivity when the temperature is modified has also been explored. Without illumination the crystals that show photoresistance at $T = 298$ K exhibit a semiconducting-like behavior, increasing resistivity when temperature is diminished, as can be seen in the inset of Fig. 5a. At temperatures $200\,\mathrm{K} \lesssim T \leqslant 298\,\mathrm{K}$, the curves can be well fitted with the expression $\rho \propto e^{\varepsilon_2/k_B T}$ where ε_2 is the energy difference between shallow donors levels created by oxygen vacancies, V_O, and the bottom of the conduction band [38]. For sample S3 a value of $\varepsilon_2 \simeq 60$ meV is obtained, while for samples S2 and S1 ε_2 gives 200 meV and 300 meV respectively. From this discussion, we assert that an increase in the V_O concentration (which is

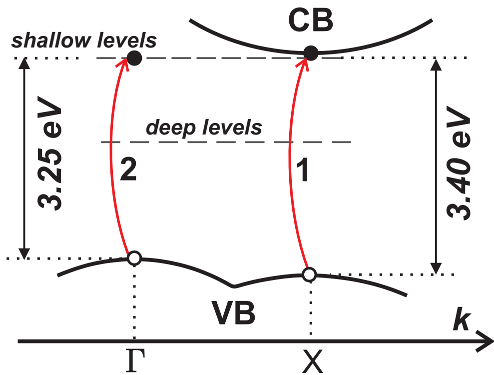

FIG. 4. Sketch of the STO energy diagram. VB and CB denote the valence and conduction band respectively. A direct transition of 3.40 eV (labeled as 1 and represented by a solid arrow) between the maximum of the VB and the minimum of the CB is attained at the X point. An indirect transition of 3.25 eV (labeled as 2 and also represented by a solid arrow) takes place between the maximum of the VB at the point Γ and the minimum of the CB at the X point.

higher for samples with higher carrier densities) decreases ε_2 thereby increasing the closeness of these levels to the minimum of the conduction band. Considering the capture cross-section of defects, $S = \pi.r^2$, and that r can be expressed in terms of the Coulomb energy $E = e^2/K.r$, where K is the dielectric constant of STO [24], it is possible to compare the capture cross-section of these shallow donor levels, S_{V_O} (with an energy $\varepsilon_2 \simeq 200$ meV for sample S2) with the one corresponding to the V_{Ti-O} deep-level traps mentioned above (which have an estimated energy of $E_t \simeq 0.86$ eV for sample S2), resulting in a

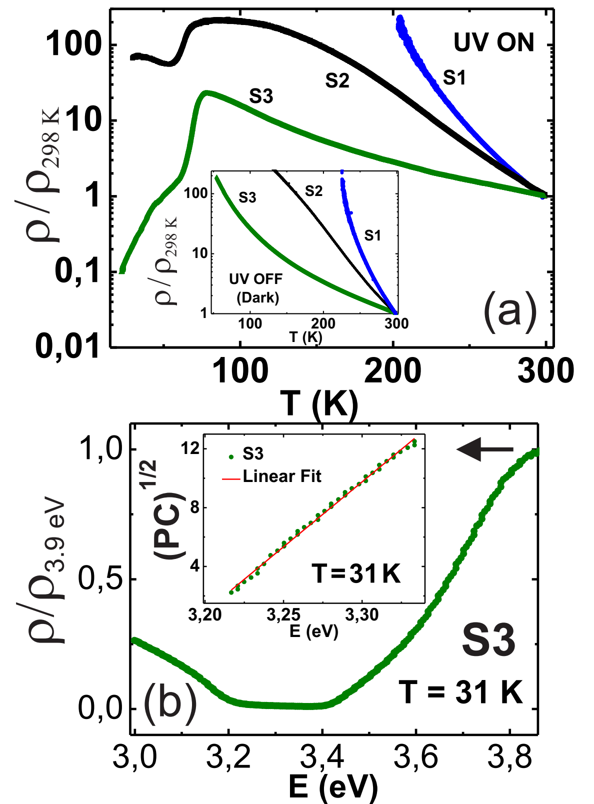

FIG. 5. a) Resistivity (normalized at its room-temperature value) as a function of temperature under the application of an incident light of $\lambda = 365$ nm. The curves correspond to the sample S1 (blue circles), S2 (black squares) and S3 (green triangles). For sample S1, resistivity measurements below ~ 200 K are above our instrument range. Inset: Resistivity (normalized at its room-temperature value) without illumination as a function of temperature for the STO crystal S1 (blue circles), S2 (black squares) and S3 (green triangles). b) Resistivity (normalized at its 3.9 eV value) as a function of the incident light energy for the sample S3 at $T = 31$ K. The arrow marks the direction of the scan (denoted in this case as H-L scan). The scanning speed of the incident light wavelength was $0.1\,\mathrm{nm\,s^{-1}}$. Instead of a minimum, a plateau is observed between ~ 3.40 eV and ~ 3.25 eV. Inset: Photocurrent, PC, as a function of the incident light energy for the L-H scan. The data follows a $PC^{1/2}$ dependence with the energy.

ratio $S_{V_O}/S_{V_{Ti-O}} \simeq 19$. This estimation indicates that the capture cross-section due to the exceeding V_O's is at least one order of magnitude higher than the one corresponding to V_{Ti-O}'s confirming that the V_O's are able to screen the V_{Ti-O}'s decreasing in this way their capabilities as trapping centers as V_O density is increased above the V_{Ti-O} concentration.

When illumination is applied, the results are remarkably different, see main panel of Fig. 5a. A metal-insulator transition (MIT) induced by light takes place around $T \sim 85\,$K for the samples S2 and S3 and it is more pronounced for the latter crystal. Resistivity measurements in sample S1 below $\sim 200\,$K are above our instrument range. At first sight, this drop of resistivity can be due to an enhancement of carrier mobility, μ, below the transition temperature, T_{MI}, or to a sudden increment of the promoted electrons to the conduction band when illumination is applied, $\triangle n$. It is known that carrier mobility in STO increases when temperature is diminished as $\mu \propto T^{-2.7}$ for $T \gtrsim 150\,$K and it nearly saturates below that temperature [39–41]. Consequently, an increment of $\triangle n$ below T_{MI} seems to be taken place. As a first approximation, $\triangle n$ is proportional to the absorption coefficient, hence the photoresistance excitation spectrum at $T < T_{MI}$ can provide us useful information about the origin of this transition. In Fig. 5b a H-L scan at $T = 31\,$K is presented for sample S3, but similar curves have been observed for the crystal S2 at that temperature. Again, we have chosen a scanning speed below which all the scanning curves are equal within our experimental resolution. The L-H scans at this temperature are very similar to the ones higher temperatures, see Fig. 3a, with a maximum slope at $(3.25 \pm 0.04)\,$eV confirming in this way that at low temperatures the indirect gap is still efficient to produce photoelectrons. If after this sweep the H-L scan is performed at $T = 31\,$K, instead of the $\sim 3.40\,$eV minimum found in the higher temperatures H-L scans, a plateau is observed between $(3.40 \pm 0.03)\,$eV and $(3.25 \pm 0.04)\,$eV, see Fig. 5b. While the direct transition at $\sim 3.40\,$eV still seems to play an important role in the photoresistivity at low temperatures, it is also evident that the indirect gap has become a more efficient mechanism to generate photoelectrons at these temperatures, just compare this H-L scan with the one at higher temperatures where at $\sim 3.25\,$eV the recombination rate was dominant and the resistivity was already increasing, see Fig. 3b.

Since the $\sim 3.25\,$eV gap is an indirect one, the transference of photo-electrons from the top of the valence band to the bottom of the conduction band is assisted by a phonon. Several experiments like optical absorption [4], Raman spectroscopy [42], photoluminescence [17] and tunneling [43] confirm the appearance of a longitudinal optical phonon at $T < 77\,$K that might be the responsible of this enhanced efficiency of the indirect gap. On the other hand, it is well established that STO experiences a cubic to tetragonal transition at $T \simeq 105\,$K [44–46], and it has been proposed that it will produce a folding of the Brillouin zone (BZ) that would affect the $\sim 3.25\,$eV indirect gap converting it in a direct one with the same energy for $T < 105\,$K [47, 48], thereby increasing $\triangle n$ at low temperatures. Considering that the photocurrent, PC, is proportional to the absorption coefficient [24, 49], we have found that the L-H scan at $T < T_{MI}$ follows a $PC^{1/2}$ dependence with the incident light energy (see inset of Fig. 5b) concomitant with the presence of an indirect gap at these temperatures [4, 50]. Hence, the gap conversion effect due to the BZ folding is not a plausible scenario.

In summary, we report a systematic photoresistivity study in reduced STO single crystals. Indirect and direct gap transitions with the intervention of trapping defects are responsible of the room-temperature persistent photoresistance. A metal-insulator transition induced by light has been observed at $T \simeq 85\,$K probably related to the appearance of an efficient phonon that can mediate the indirect gap transition at low temperatures. Our results can help to understand the noteworthy photoresistance observed in bilayers based in STO crystals at room-temperature [8] but also at low temperatures [9, 26].

G. B. thanks K. Behnia, B. Fauqué and X. Lin for motivating our research on STO. G. B. and M. V. acknowledge the support from CONICET-Argentina. This work was supported by CIUNT under Grant No. 26/E530. We acknowledge to the SNMAG facilities.

[1] J. Heber, Nature **459**, 28 (2009).
[2] H. Y. Hwang, Y. Iwasa, M. Kawasaki, B. Keimer, N. Nagaosa and Y. Tokura, Nature Materials **11**, 103 (2012).
[3] M. Cardona, Phys. Rev. **140**, A651 (1965).
[4] M. Capizzi and A. Frova, Phys. Rev. Lett. **25**, 1298 (1970).
[5] A. Ohtomo and H. Y. Hwang, Nature **427**, 423 (2004).
[6] S. Thiel, G. Hammerl, A. Schmehl, C. W. Schneider and J. Mannhart, Science **313**, 1935 (2006).
[7] M. Huijben, G. Rijnders, D. H. A. Blank, S. Bals, S. van Aert, J. Verbeeck, G. van Tendeloo, A. Brinkman, and H. Hilgenkamp, Nature Materials **5**, 556 (2006).
[8] A. Tebano, E. Fabbri, D. Pergolesi, G. Balestrino and E. Traversa, ACS Nano **6**, 1278 (2012).
[9] H.-L. Lu, Z.-M. Liao, L. Zhang, W.-T. Yuan, Y. Wang, X.-M. Ma and D.-P. Yu, Scientific Reports, **3**, 2870 (2013).
[10] H. Yasunaga and I. Nakada, J. Phys. Soc. Japan **22**, 338 (1967).
[11] M. C. Tarun, F. A. Selim and M. D. McCluskey, Phys. Rev. Lett. **111**, 187403 (2013).
[12] H.-H. Nahm, C. H. Park and Y.-S. Kim, Scientific Re-

ports **4**, 4124 (2014).
[13] D. A. Muller, N. Nakagawa, A. Ohtomo, J. L. Grazul and H. Y. Hwang, Nature **430**, 657 (2004).
[14] A. Spinelli, M. A. Torija, C. Liu, C. Jan and C. Leighton, Phys. Rev. B **81**, 155110 (2010).
[15] J. F. Schooley, W. R. Hosier, E. Ambler and J. H. Becker, Phys. Rev. Lett. **14**, 305 (1965).
[16] X. Lin, Z. Zhu, B. Fauqué and K. Behnia, Phys. Rev. X **3**, 021002 (2013).
[17] L. Grabner, Phys. Rev. **177**, 1315 (1969).
[18] A. Janotti, J. B. Varley, M. Choi and C. G. Van de Walle, Phys. Rev. B **90**, 085202 (2014).
[19] D. Rubi, S. Duhalde, M. C. Terzzoli, M. Villafuerte, Applied Surface Science **197**, 536 (2002).
[20] X. Lin, G. Bridoux, A. Gourgout, G. Seyfarth, S. Krämer, M. Nardone, B. Fauqué and K. Behnia, Phys. Rev. Lett. **112**, 207002 (2014).
[21] A. Müller and K. H. Härdtl, Appl. Phys. A **49**, 75 (1989).
[22] H. -J. Schlüter, M. Barsoum and J. Maier, Solid State Ionics **101**, 509 (1997).
[23] C. Tragut and K. H. Härdtl, Sens. Act. B **4**, 425 (1991).
[24] R. H. Bube, *Photoconductivity of Solids*, (John Wiley & Sons, New York, 1960).
[25] D. Comedi, S. P. Heluani, M. Villafuerte, R. D. Arce and R. R. Koropecki, J. Phys.: Condens. Matter **19**, 486205 (2007).
[26] K. X. Jin, W. Lin, B. C. Luo and T. Wu, Scientific Reports **5**, 8778 (2015).
[27] R. H. Bube, *Photoelectronics Properties of Semiconductors*, (Cambridge University Press, Cambridge, 1992).
[28] S. A. Studenikin, N. Golego and M. Cocivera, J. Appl. Phys. **83**, 2104 (1998).
[29] N. Shanthi and D. D. Sarma, Phys. Rev. B **57**, 2153 (1998).
[30] T. Higuchi, T. Tsukamoto, K. Kobayashi, Y. Ishiwata, M. Fujisawa, T. Yokoya, S. Yamaguchi and S. Shin, Phys. Rev. B **61**, 12860 (2000).
[31] Y. Ishida, R. Eguchi, M. Matsunami, K. Horiba, M. Taguchi, A. Chainani, Y. Senba, H. Ohashi, H. Ohta and S. Shin, Phys. Rev. Lett. **100**, 056401 (2008).
[32] T. Tanaka, K. Matsunaga, Y. Ikuhara and T. Yamamoto, Phys. Rev. B **68**, 205213 (2003).
[33] R. A. Mackie, S. Singh, J. Laverock, S. B. Dugdale and D. J. Keeble, Phys. Rev. B **79**, 014102 (2009).
[34] C. Lee, J. Destry and J. L. Brebner, Phys. Rev. B **11**, 2299 (1975).
[35] W. D. Rice, P. Ambwani, M. Bombeck, J. D. Thompson, G. Haugstad, C. Leighton and S. A. Crooker, Nature Materials **13**, 481 (2014).
[36] W. P. Dumke, Phys. Rev. **105**, 139 (1957).
[37] Y. Yamada and Y. Kanemitsu, Phys. Rev. B **82**, 121103(R) (2010).
[38] N. Mott and E. Davis, *Electronic Processes in Non-Crystalline Materials*, 2nd ed. (University Press, Oxford, 1979).
[39] O. N. Tufte and P. W. Chapman, Phys. Rev. **155**, 796 (1967).
[40] C. Lee, J. Yahia and L. Brebner, Phys. Rev. B **3**, 2525 (1971).
[41] J. Son, P. Moetakef, B. Jalan, O. Bierwagen, N. J. Wright, R. Engel-Herbert and S. Stemmer, Nature Materials **9**, 482 (2010).
[42] W. G. Nilsen and J. G. Skinner, J. Chem. Phys. **48**, 2240 (1968).
[43] S. Shapiro, Phys. Rev. **140**, A169 (1965).
[44] P. A. Fleury, J. F. Scott and J. M. Worlock, Phys. Rev. Lett. **21**, 16 (1968).
[45] E. Courtens, Phys. Rev. Lett. **29**, 1380 (1972).
[46] M. Kisiel *et al.*, Phys. Rev. Lett. **115**, 046101 (2015).
[47] H. Unoki and T. Sakudo, J. Phys. Soc. Jap. 28, 546 (1967).
[48] E. Heifets, E. Kotomin and V. A. Trepakov, J. Phys.: Condens. Matter **18** 4845 (2006).
[49] J. I. Pankove, *Optical Processes in Semiconductors*, (Dover Publications Inc., 1976).
[50] A. M. Fox, *Optical Properties of Solids*, (Oxford University Press, London, 2010).